

The sensors for the intelligent micro washing system
Sensor array 1: The measurements

Work report 9, 13-Feb-97
Geert Langereis

1. Introduction	2
2. Measurements using the integrated sensor array	3
2.1 Conductivity.....	3
2.2 Chrono amperometry	7
2.3 Temperature	8
3. Measurements using the multipurpose sensor structure	11
3.1 Conductivity.....	11
3.2 Chrono amperometry	13
3.3 Temperature	14
4. Conclusions.....	15
A. References.....	16

1. Introduction

This report contains the measurement results using the “integrated sensor array” and the “multi purpose sensor” as described in work report 8. The idea is to use an array consisting of three basic elements which will be used to measure three basic parameters directly. In addition, by using these basic elements together or just after each other, some new parameters will probably be found. In this report, only the testing of the basic elements operation is presented.

The three basic elements which were implemented are:

1. A two-points conductivity cell;
2. A working electrode for amperometric measurements and local pH control;
3. A resistor for thermoresistive measurements and heating.

These elements were implemented in two ways:

- As an *integrated sensor array*. This device consists of the three mentioned elements placed on a single chip, the elements can be accessed separately using six pads. The active sensing area is about $1.5 \times 2.2 \text{ mm}^2$. Three different designs for the conductivity cell resulted in three different integrated sensor arrays numbered 1, 2 and 3. The measurement results are in chapter 2.
- As a *multi purpose sensor structure*. This device gives the possibility to access all three basic elements in a single structure using four connecting pads. Two dimensions were implemented resulting in multi purpose sensor structure A and B. The measurement results are in chapter 3.

In addition, some structures were made for calcium hydroxide deposition measurements (as described in the previous work report), numbered I, II and III, and for temperature sensor-actuator research, numbered T1, T2 and T3. These 11 different sensors need to be tested according to Table 1.1.

Table 1.1: Measurements to do

Device	Description	Measurements	Using
1, 2, 3	Integrated sensor arrays	- Resistance vs. temperature - Impedance vs. conductivity - Chrono amperometry	1, 2 or 3 1, 2 and 3 1, 2 or 3
A, B	Multi purpose sensor structures	- Resistance vs. temperature - Impedance vs. conductivity - Chrono amperometry	A and B A and B A and B
I, II, III	Conductivity sensors for $\text{Ca}(\text{OH})_2$ deposition purposes	- Impedance before and after applied current in calcium solution	I, II and III
T1, T2, T3	Dual thermoresistive structures	- Temperature while heating with the other	T1, T2, T3

Because devices I-III and T1-T3 are for the advanced purposes, their use will be reported in future.

2. Measurements using the integrated sensor array

This chapter reports the measurements of the three basic sensor elements which are implemented in the integrated sensor array. Although they were realised on a single chip, they are measured separately.

2.1 Conductivity

Short theory

The conductivity cell is a two points one, implemented as an interdigitated structure. As evaluated in work report 8, the impedance $Z(\omega)$ between the frequencies

$$f_{lo} = \frac{\kappa_{sol}}{\pi W L N C_{char} K_{Cell}} \approx \frac{1}{\pi R_{Sol} C_{Interface}} \quad (2.1)$$

and

$$f_{hi} = \frac{\kappa_{sol}}{2\pi\epsilon_0\epsilon_{sol}} \approx \frac{1}{2\pi R_{Sol} C_{Cell}} \quad (2.2)$$

is equal to:

$$Z(\omega) = 2R_{Lead} + R_{Sol} = 2R_{Lead} + \frac{K_{Cell}}{\kappa_{Sol}} \quad (2.3)$$

with the equivalent circuit parameters:

- R_{Sol} : resistance of the electrolyte,
- $C_{Interface}$: influence of the interface capacitance,
- C_{Cell} : cell capacitance,
- R_{Lead} : resistance of the connecting leads,

and the geometrical and physical parameters:

- W : width of the fingers,
- L : length of the fingers,
- N : number of fingers,
- K_{Cell} : cell constant containing only W , L and N ,
- ϵ_0 : dielectric constant,
- ϵ_{Sol} : relative dielectric constant of water ($\gg 80$),
- κ_{Sol} : conductivity of the electrolyte,
- C_{char} : interface capacitance per square unit.

Three sets of parameters were chosen as given in Table 2.1. It can be seen that the theoretical working area lies between $f_{lo} = 4 - 10$ kHz and $f_{hi} = 1.1$ GHz for a conductivity of $500 \mu\text{S/cm}$.

Table 2.1: Chosen parameters for the conductivity cell, the temperature resistor and the working electrode, with the resulting theoretical model parameters at 20°C.

	Type 1	Type 2	Type 3
Conductivity			
S [μm]	15	5	115
W [μm]	100	200	115
L [μm]	1035	1025	1155
N	9	5	5
C_{Cell} [pF]	5.29	3.48	1.64
R_{Sol} [k Ω] *	2.68	4.08	8.66
R_{Lead} [Ω]	1	1	1
C_{Int} [nF]	13.04	14.36	9.30
K_{Cell} [m^{-1}]	134	204	433
f_{lo} [kHz] *	9.10	5.50	3.95
f_{hi} [GHz] *	1.12	1.12	1.12
Temperature			
L_{T} [mm]	14	14	14
W_{T} [μm]	10	10	10
$R_{20^\circ\text{C}}$ [W]	560	560	560
Working electrode			
A [mm^2]	2×0.50	2×0.50	2×0.40

* For $\kappa_{\text{Sol}} = 500 \mu\text{S/cm}$

The parameters which were not mentioned yet are:

- S Space between the fingers of the conductivity cell;
- L_{T} Effective length of the resistive path (for temperature measurements);
- W_{T} Width of the resistive path (for temperature measurements);
- $R_{20^\circ\text{C}}$ Resistance at 20°C;
- A Effective area for working electrode purposes.

Experimental

The measurements were carried out using a Hewlett Packard impedance/gain-phase analyzer type HP4194A, controlled by a computer using the graphical programming environment HP VEE.

The temperature of the sample was 21°C. Impedance versus frequency sweeps were made for sensors 1, 2 and 3 in 0.5, 1.0, 5.0 and 10 mM KNO_3 (equal to conductivities of about 62, 120, 600 and 1200 $\mu\text{S/cm}$). The amplitude of the oscillator voltage was 100 mV.

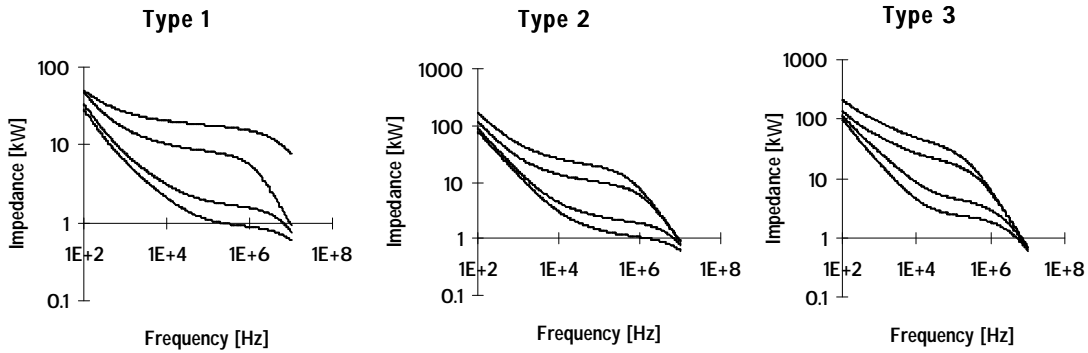


Figure 2.1: Impedance versus frequency sweeps for the integrated sensor arrays
From top to bottom: 0.5, 1.0, 5.0 and 10 mM KNO_3

Figure 2.1 shows the results. The lower and upper frequency bounds as given by equations (2.1) and (2.2) can be found from the typical shape of the impedance curves. At a frequency of 500 kHz all three figures show a plateau at which the impedance is a measure for the conductivity according to equation (2.3). Figure 2.2 shows the measured admittance at KNO_3 concentrations from 0.50 to 100 mM (equivalent to conductivities of about 62 $\mu\text{S}/\text{cm}$ to 10 mS/cm).

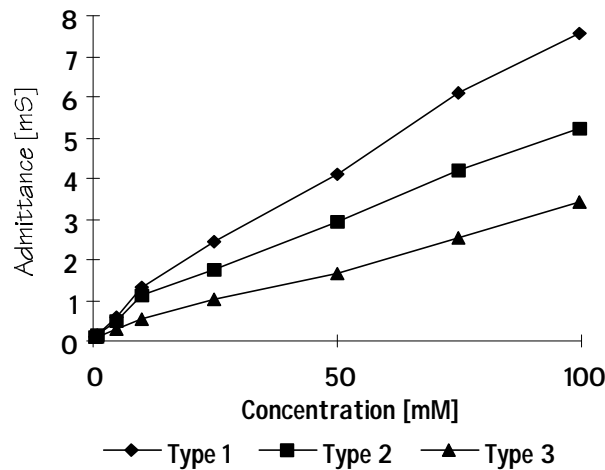


Figure 2.2: Measured admittance at 500 kHz

Data evaluation

It can be seen from Figure 2.1 that the frequency boundaries are concentration dependent. Actually, the operational frequency should be chosen according to the conductivity, since it is not possible to measure conductivity over several decades at a single operational frequency (see the not ideal shape of Figure 2.2). This problem can simply be solved by using an operational frequency which is dependent on the measurement range (most commercial conductivity meters uses this).

A more accurate method, is to find the frequency at the deflection points (where the second derivative is equal to zero) in the impedance plot. This will be the frequency where the influence of C_{Cell} and $C_{\text{Interface}}$ is minimal. Figure 2.3 shows that this method indeed results into a more linear relation.

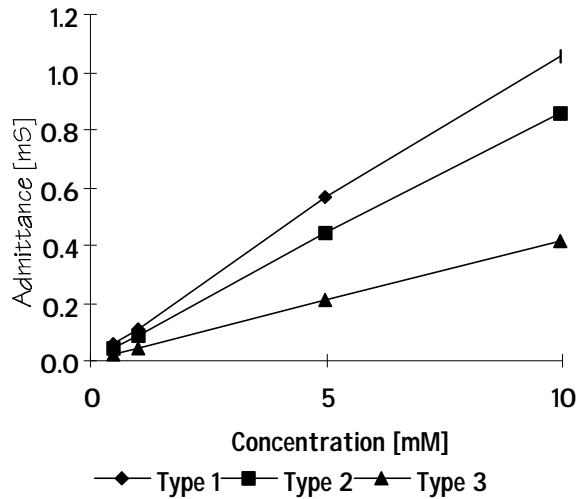


Figure 2.3: Admittance at the deflection points (not necessarily 500 kHz) of Figure 2.1 versus KNO_3 concentration

Using this graph, the cell constants can be determined. The translation from KNO_3 concentration to the actual conductivity was done by measuring the conductivity using a Consort K820 conductivity meter.

Table 2.2: Translation from KNO_3 concentration to conductivity

Concentration [mM]	Conductivity [mS/cm]
0.5	0.0716
1.0	0.143
5.0	0.681
10.0	1.264

Table 2.3 summarises the found cell constants which can be compared to the theoretical cell constants of Table 2.1.

Table 2.3: Measured conductivity parameters

	Type 1	Type 2	Type 3
$K_{\text{Cell}} [\text{cm}^{-1}]$	1.24	1.56	3.31
$f_{\text{lo}} [\text{kHz}]^*$	3.34	6.57	5.55
$f_{\text{hi}} [\text{MHz}]^*$	3.74	3.50	1.94
$C_{\text{Char}} [\mu\text{F}/\text{cm}^2]$	9.74	3.67	3.88
$C_{\text{Cell}} [\text{pF}]$	25.1	18.6	16.7
$R_{\text{Sol}} [\text{k}\Omega]^*$	1.77	2.26	4.76
$C_{\text{Interface}} [\text{nF}]$	45.4	18.8	12.9

* at a conductivity of $681 \mu\text{S}/\text{cm}$

The boundary frequencies f_{lo} and f_{hi} can be fitted from the impedance plots by determining the intersections of the slope lines. The interface capacitance per square unit C_{Char} and equivalent electrical components can now be calculated using equation (2.1) and (2.2). The results are in the lower rows of Table 2.3.

Conclusions

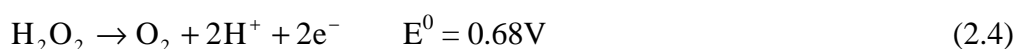
It can be seen that only the upper frequency limit differs much from the theoretical value, which results in a much larger equivalent circuit cell capacitance C_{Cell} . The

reason for this is probably that the unshielded connecting wires of the devices have a capacitance of some pico-Farads, this results in a parasitic capacitance parallel to C_{Cell} . The tested measurement range of $62 \mu\text{S}/\text{cm}$ to $10 \text{mS}/\text{cm}$ (Figure 2.2) is suitable for the conductivity of tap water ($100 - 900 \mu\text{S}/\text{cm}$) and during washing (about $2 \text{mS}/\text{cm}$). For increasing accuracy either a non-linear calibration curve, or the method using the deflection point analysis can be used.

2.2 Chrono amperometry

Short theory

The primary aim of the working electrode is to measure bleach activity using chrono-amperometry. Hydrogen peroxide is chosen here as a bleaching agent. The reaction involved is:



which occurs at a positive potential step. The theoretical current response is given by the Cottrell equation:

$$i(t) = nFA C_{\text{H}_2\text{O}_2} \sqrt{\frac{D_{\text{H}_2\text{O}_2}}{\pi t}} \quad (2.5)$$

with F the Faraday constant, n the number of electrons transferred, A the actuator area, $C_{\text{H}_2\text{O}_2}$ the bulk H_2O_2 concentration and $D_{\text{H}_2\text{O}_2}$ the diffusion coefficient (approximately $1.6 \cdot 10^{-5} \text{cm}^2/\text{sec}$ at $\text{pH} < 10$ [1]).

Experimental

The chrono amperometric experiments were carried out using the working electrode of a type 1 sensor (0.50mm^2) in a three electrode set-up with an Ag/AgCl reference electrode and a platinum counter electrode. The measurement set-up consisted of an EG&G potentiostat/galvanostat model 173 under computer control.

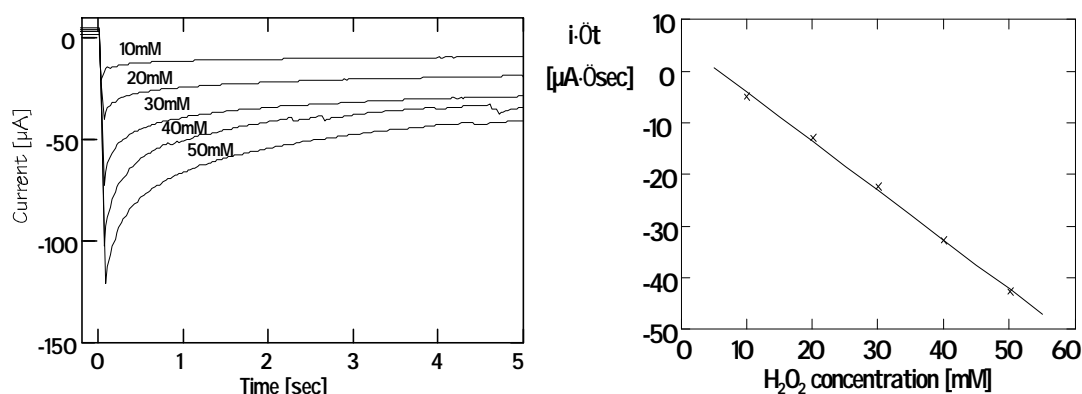


Figure 2.4: Chrono amperometric H_2O_2 measurements

Hydrogen peroxide concentrations were used of 10, 20, 30, 40 and 50 mM, directly measured after dilution from a 80wt% bulk solution. To prevent an ohmic drop across the sample, a background electrolyte of 10mM KNO_3 was used.

Figure 2.4 (left) shows the recorded current responses which show the characteristic i/\sqrt{t} shape. A potential step of 1 Volt versus Ag/AgCl appeared to be sufficient for satisfying the Cottrell conditions.

Data evaluation

Figure 2.4 (right) was constructed from the left figure by plotting the recorded current versus i/\sqrt{t} and determining the slope. These slopes as a function of the H_2O_2 concentration gives the calibration curve for the sensor.

From equation (2.5) the diffusion coefficient of hydrogen peroxide can now be determined. The slope of Figure 2.4 (right) is equal to $0.955 \mu A \cdot sec^{1/2} \cdot mM^{-1}$, which results in:

$$D_{H_2O_2} = \pi \left(\frac{\text{slope}}{nFA} \right)^2 = 1.23 \cdot 10^{-5} \cdot cm^2 \cdot sec^{-1}$$

which is in the range of the mentioned $1.6 \cdot 10^{-5} cm^2/sec$ [1].

Conclusions

Chrono amperometry appears to be a reliable method for the detection of a hydrogen peroxide solution. The tested concentration range covers the actual values during washing. Because the bleaching process is the reduction of stains, this method measures the actual bleach activity.

There are some small problems for implementing this technique in a miniaturised sensor system. First the used glass reference electrode does not suit the aim of integration of sensors. Because it does not influence the measured current directly, this reference might be simplified in future. The second problem is the square root operation required to interpret the data. In a microcontroller system this operation will take a lot of memory and processor time.

2.3 Temperature

Short theory

The resistance of a metal strip is:

$$R_0 = \frac{\rho l}{wh} \quad (2.6)$$

where w the width, h the thickness and l the length of the strip and ρ the specific resistivity of the metal. For platinum, the resistivity at room temperature is $1.0 \cdot 10^{-5} \Omega \cdot cm$. The used structure has an intended thickness of 250 nm, a width of 10 μm and a length of 14 mm. Therefore, the nominal resistance will be 560 Ω .

The change in resistance due to temperature can be written as:

$$R = R_0 (1 + \alpha(T - T_0)) \quad (2.7)$$

with α the temperature coefficient. This coefficient is $0.00392 \text{ } ^\circ C^{-1}$ for platinum with a non-linearity of 0.2% between 0-100 $^\circ C$ [2].

Experimental

Using an automated set-up the resistance versus temperature was recorded. The set-up consisted of a Radiometer CDM210 conductivity meter used to measure the resistance. This meter has also the possibility to measure temperature. The set-up was controlled using the graphical programming environment LabView 3.1 for high reproducibility.

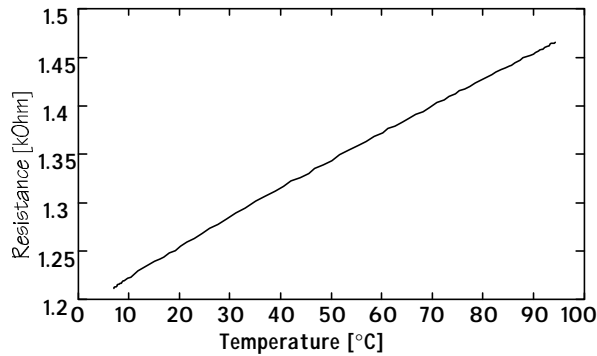


Figure 2.5: Measured resistance versus temperature

The sensor and the reference temperature electrode were placed in a glass of water with ice on a heater with stirring option. The measurement as shown in Figure 2.5 was constructed by recording both the sensor resistance and the reference temperature while heating the water.

Data evaluation

At 20°C the resistance of the sensor is equal to 1.255 kW. This is more than twice as large as the theoretical 560 W. To verify whether the intended metal layer thickness of 250 nm was realised, a surface scan was made using the Dektak surface profiler (Figure 2.6).

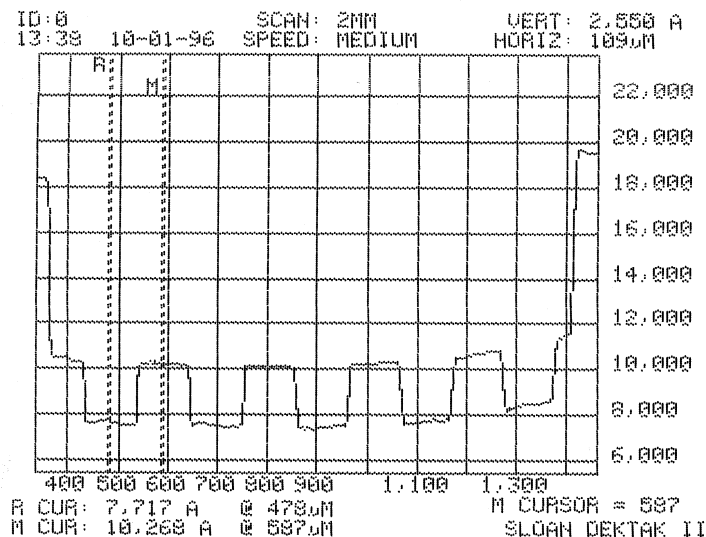


Figure 2.6: Dektak surface profiler output for a sensor of type 3

The scan was made across the interdigitated structure part of a sensor of type 3. From the left to the right there is an 850 nm thick polyimide layer, N = 5 fingers and another

polyimide layer. The thickness of the fingers is 255 nm determined by the cursors “R” and “M”. So the measured resistance should be lower according to this.

Probably the complete deviation can be subscribed to the adhesive tantalum layer, forming a tantalum-platinum alloy (tantalum has a much lower resistance than platinum).

After choosing a reference temperature, the temperature coefficient α can be found using equation (2.7). For a reference temperature of $T_0 = 20^\circ\text{C}$, the found value is: $\alpha = 0.00231^\circ\text{C}^{-1}$ with an error of less than 0.5% in the worst case.

2.4 Conclusions

In the integrated sensor array, three basic elements were implemented and measured separately.

Conductivity was measured using an interdigitated structure in the range of 62 $\mu\text{S}/\text{cm}$ to 10 mS/cm which is adequate for the washing environment. The linearity of the calibration plot using a single operational frequency can be increased by improving the control logic.

The hydrogen peroxide concentration was measured as being representative for all possible bleaching compounds. In a three electrode set-up using a potentiostat, the result was satisfying. Attention should be paid to implementing this advanced laboratory control system into a more simple read out system.

The measurement of temperature in the desired range turned out to be very simple using the thermoresistive effect of platinum. This method showed high linearity and can be implemented very simple.

The complete chips are $3 \times 4 \text{ mm}^2$ and have an active area of $1.5 \times 2 \text{ mm}^2$. The number of connecting pads is six, but this will be reduced to four in the next chapter.

3. Measurements using the multipurpose sensor structure

This chapter has the same structure as the previous one, but now the measurements are done using the multi purpose sensor structures.

3.1 Conductivity

Short theory

The two different multi purpose sensor structures were constructed from sensor arrays 1 and 2 by cutting the fingers of the interdigitated structure along (Figure 3.1).

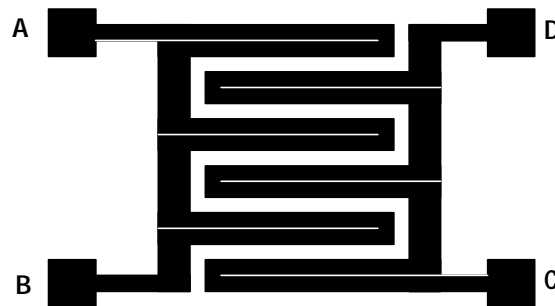


Figure 3.1: The multi purpose sensor concept:
 Conductivity: Impedance between pads A, B and C, D
 Temperature: Resistance between pads A and B (or C and D)
 Working electrode: A, B, C and D versus external counter electrode

When both pads A-B and C-D are short cut, the structure can be used as an interdigitated structure with the dimensions as in Table 3.1.

Table 3.1: Chip lay-outs for the integrated sensors

Type A	Type B
Conductivity	
S = 5 μm	S = 15 μm
W = 200 μm	W = 100 μm
L = 1025 μm	L = 1035 μm
N = 5	N = 9
Temperature	
L = 10.25 mm (2 \times)	L = 8.28 mm (2 \times)
W = 47 μm	W = 45 μm
R = 87 W	R = 87 W
Working electrode	
A = 2 \times 0.48 mm ²	A = 2 \times 0.42 mm ²
Active area	
A = 1.025 \times 1.025 mm ²	A = 1.035 \times 1.035 mm ²

Experimental

The measured impedance versus frequency plots are in Figure 3.2. The electrolyte was KNO_3 with concentrations of 0.5, 1, 5 and 10 mM. The room temperature was 20°C .

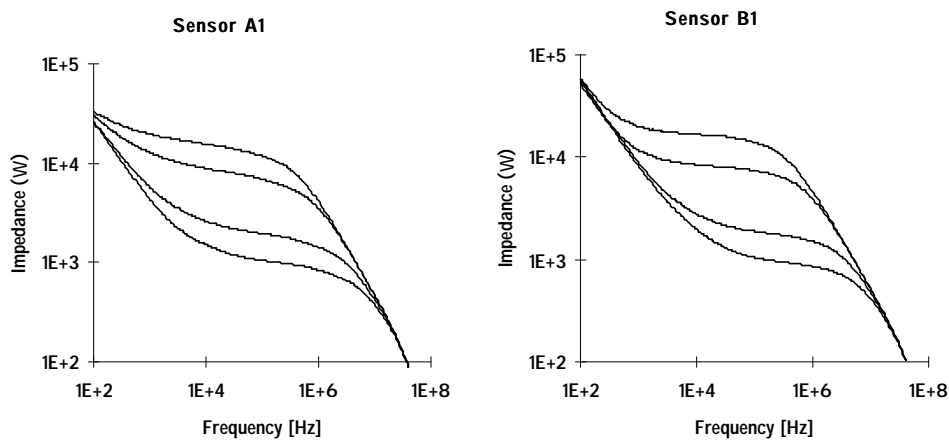


Figure 3.2: Impedance versus frequency sweeps for the multi purpose sensor structures
From top to bottom: 0.5, 1.0, 5.0 and 10 mM KNO_3

Data evaluation

In order to compare the data to the normal interdigitated cells, the results are plotted in Figure 3.3 together with the data of the sensors 1, 2 and 3 as already presented in Figure 2.3.

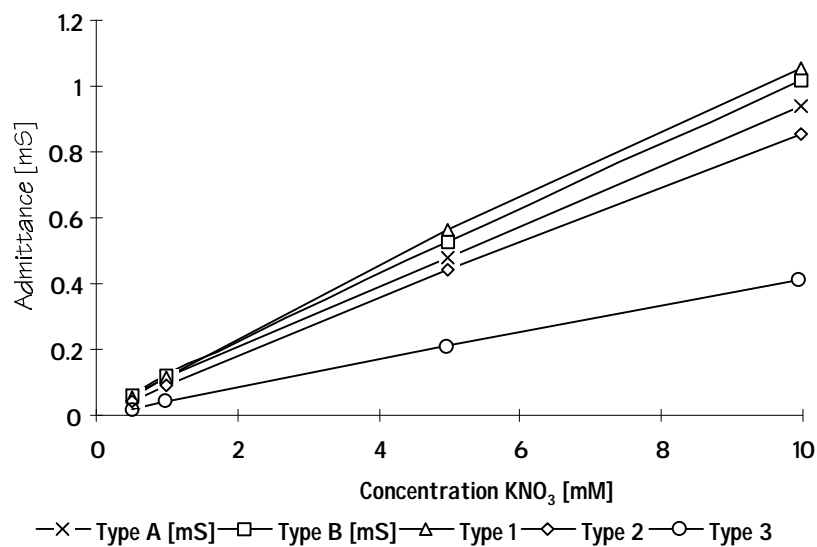


Figure 3.3: Measured admittance at the deflection points of Figure 3.2 versus KNO_3 concentration

Conclusions

Obviously, the linearity of the admittance versus concentration plot remains unaffected when the fingers are cut along to create the multi purpose structures. Although Figure 3.3 was made using the fitting of deflection points, from Figure 3.2 it can be concluded that a constant operational frequency of 500 kHz seems to be suitable for measuring conductivity over about two decades.

3.2 Chrono amperometry

Experimental

The amperometric experiments as carried out in the section 2.2 were repeated using the multi purpose structures. By connecting all four pads, working electrode areas are available of 0.96 and 0.84 mm² for device type A and B respectively.

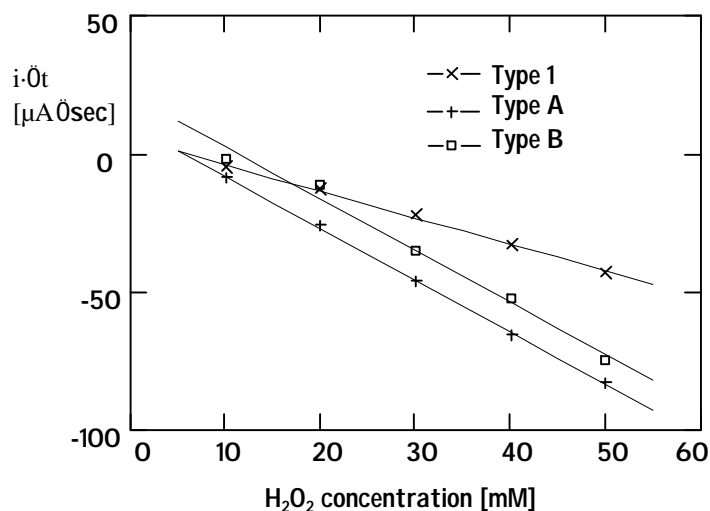


Figure 3.4: Chrono amperometric H₂O₂ measurements

In Figure 3.4 the measured calibration curves are plotted. The result for sensor type 1 (surface of A = 0.50 mm²) is repeated here as a reference.

Data evaluation

The slopes of the lines in Figure 3.4 are presented in Table 3.2. Obviously, the difference in the slopes matches the difference in the electrode surface.

Table 3.2: Measured sensitivity and electrode surface

Sensor	Slope [$\mu\text{A}\cdot\text{sec}^{1/2}\cdot\text{mM}^{-1}$]	Area [mm ²]
Type 1	0.955	0.50
Type A	1.875	0.96
Type B	1.869	0.84

Conclusions

The structure can be used to do amperometric measurements by connecting all four pads. Although the Cottrell equation is actually derived for infinitely large flat electrodes, it appears to be still valid for these devices because the measurements are in agreement with the theory.

3.3 Temperature

Theory

The theoretical resistances of the temperature sensors type A and B are 87 W and 74 W respectively. Both sensor types include two identical resistive paths, only one is being measured.

Experimental

For the resistances of structures A and B at 20°C the values of 178.4W and 85.5W were found respectively.

The measurements were performed in the same way as described before. Figure 3.5 shows the results for two type 1 sensors, two type A sensors and two type B sensors. The curves are normalised to the values at 20°C.

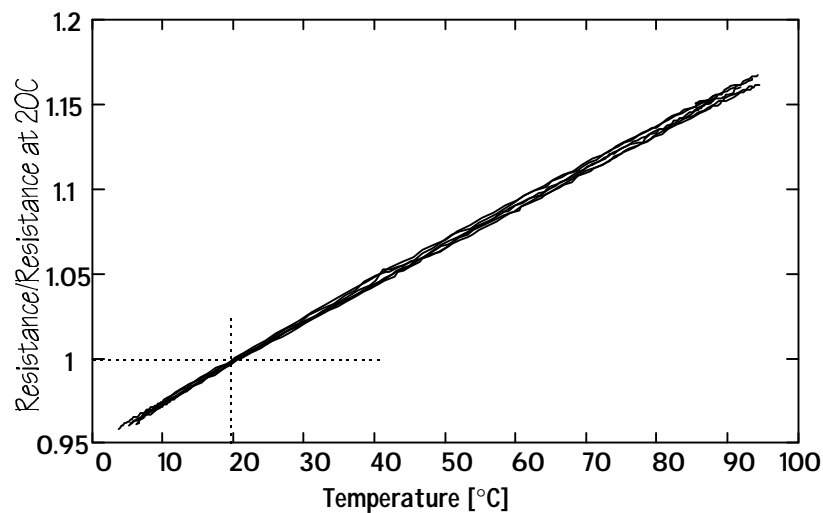


Figure 3.5: Normalised resistances versus temperature

Data evaluation and conclusion

The curves show an impressive similarity. Apparently, the temperature coefficient of $a = 0.00231^{\circ}\text{C}^{-1}$ can be used for all sensor structures.

3.4 Conclusions

It is remarkable that the results using the multi purpose devices do not differ significantly from the results using the optimised integrated array devices of chapter 2. So the number of connecting pads can be reduced from six to four without losing reliability.

Using the multi purpose structure, the simultaneous measurement is slightly more difficult. It should be questioned whether this simultaneous approach is necessary (for example to find other parameters) or a scheduling system is adequate.

4. Conclusions

The integrated sensor array “array 1” includes the following basic structures:

- a working electrode;
- an interdigitated structure;
- a thermoresistive resistor.

Two versions were designed: an integrated array version and a multi purpose structure version.

The parameters were measured separately in environments which were optimised for checking that single parameter.

- Temperature can be measured using a thermoresistive resistor. Both the integrated array and the multi purpose sensor give an excellent linear temperature dependent resistivity. The found temperature coefficient is $\alpha = 0.00231^{\circ}\text{C}^{-1}$ with a non-linearity of less than 0.5% for a reference temperature of $T_{\text{Ref}} = 20^{\circ}\text{C}$. This was tested over the range of 10-90°C.

This highly reproducible temperature coefficient does not suit the values found in literature, probably because the platinum film has become an alloy with the underlying adhesion tantalum layer.

- At an operational frequency of 500 kHz, the integrated array and the multi purpose sensor can be used to measure conductivity. The tested measurement range of 62 $\mu\text{S}/\text{cm}$ to 10 mS/cm is suitable for the conductivity of tap water (100 - 900 $\mu\text{S}/\text{cm}$) and during washing (about 2 mS/cm). For increasing the linearity of the calibration curve, two operational frequencies or a non-linear calibration curve will be necessary. The upper limit of the useful frequency range appeared to be determined by the parasitic capacitances of the set-up.
- Using the working electrode for chrono amperometry, hydrogen peroxide can be determined. The structures were tested over a range of 10-50 mM H_2O_2 in an environment with 10 mM KNO_3 as a background electrolyte.

It is remarkable that the step from the integrated sensor array (which contains optimised sensors) to the multipurpose structure did not significantly influence the reliability of the measurements. Apparently, the boundary effects did not introduce parasitic elements.

The measurements were performed using laboratory set-ups (potentiostat, gain/phase analyser). In future attention should be paid to the optimisation for the use in a simple on-line system.

Another point of interest is the consequence of simultaneously measuring. This will include both chemical and electrical interferences.

The two available actuator functions were not mentioned in this report. In future the opportunities of controlling the local pH and heating the direct environment of the sensor will be used to get a flexible sensor-actuator device.

A. References

- [1] M.R. Bekebrede,
Literatuurstudie naar: Electroden voor het detecteren van waterstofperoxide in de tuinbouw, Rapport Universiteit Twente, faculteit CT, juni 1996.
- [2] R.S.C. Cobbold,
Transducers for biomedical measurements: principles and applications, John Wiley & sons, New York, 1974.

Distribution list:

P. Bergveld (UT BIO)

W. Olthuis (UT BIO)

A.P.A.F. Rocourt (URL)